



Iranian Research Organization  
for Science and Technology  
(IROST)

Advances  
Environmental  
Technology



Journal home page: <https://aet.irost.ir/>

# Application and comparison of the performance of multi-wall magnetic carbon nanotubes for removing paclitaxel and gemcitabine from sewage by adsorption process

Setareh Safari<sup>1</sup>, Fatemeh Nasehi\*<sup>1</sup>, Ebrahim Fataei\*<sup>1</sup>, Behnam Khanizadeh<sup>2</sup> and Ali Akbar Imani<sup>3</sup>

<sup>1</sup>Department of Environmental Science and Engineering, Ardabil Branch, Islamic Azad University, Ardabil, Iran

<sup>2</sup>Department of Chemistry, Ardabil Branch, Islamic Azad University, Ardabil, Iran

<sup>3</sup>Department of Agriculture, Ardabil Branch, Islamic Azad University, Ardabil, Iran

## ARTICLE INFO

Document Type:  
Research Paper

### Article history:

Received 5 July 2022

Received in revised form

29 November 2022

Accepted 29 November 2022

### Keywords:

Multi-walled carbon  
nanotube  
Iron oxide  
Adsorption  
Paclitaxel  
Gemcitabine

## ABSTRACT

This study investigated the performance and adsorption properties of multi-magnetic carbon nanotubes in removing paclitaxel (PTX) and gemcitabine (GEM) from industrial sewage. For this purpose, the first magnetic multi-walled carbon nanotubes were prepared by the co-sedimentation method. Their characteristics were determined by scanning electron microscopy analysis of field emission (FESEM), transmission electron microscopy (TEM), energy dispersive x-ray (EDX), X-ray diffraction (XRD), and a vibration sample magnetometer. The results showed that iron oxide nanoparticles were incorporated well without destroying the structure of the nanotubes. Also, the effect of the pH solution and adsorbent dosage on the adsorption of drugs was examined. The pH of 7 and adsorbent dosage of 200 mg/L were found to be the optimal conditions for the process. Comparing the removal results of paclitaxel and gemcitabine contaminants from the sewage showed that the multi-magnetic carbon wall nanotubes were more efficient in removing PTX (58%) than GEM (26%). Studies on the reaction kinetics and adsorption isotherms were performed on the two contaminants. The results obtained from the fitting of the curve showed that the kinetics reaction of the drugs was of the second order and consistent with the Langmuir isotherm. Finally, the reusability and stability of the adsorbent were investigated, and the reductions detected for PTX and GEM were only 8% and 5%, respectively, after five cycles.

## 1. Introduction

One of the essential components of the universe is water. Water plays a crucial role in the proper functioning of ecosystems. It is reported that there

are more than 700 types of organic and inorganic pollutants present in the world's waters, some of which are toxic, carcinogenic, and remain in the environment for a long time and are non-degradable. In the last 30 years, medicinal

\*Corresponding author: Tel.: +981333720992

E-mail: [ebfataei@iauardabil.ac.ir](mailto:ebfataei@iauardabil.ac.ir), [f.nasehi@iauardabil.ac.ir](mailto:f.nasehi@iauardabil.ac.ir)

DOI:10.22104/AET.2022.5747.1574

compounds have been considered the most important pollutants of surface water and groundwater in industrial and residential communities owing to their high diversity, high consumption, and stability in the environment [1-10]. These substances are a special group of micro-pollutants entering the environment from the effluent of the pharmaceutical industry or point sources, such as sewage and waste, and non-point sources, like agricultural runoff. Because of their complex structures, low biodegradability, and lack of any specific control in many sewages, conventional treatment systems do not completely remove the cytotoxic compounds [11-17]. Since pharmaceutical contaminants have unique physical and chemical properties, they can pass through all natural filters [18]. Therefore, they can enter the outflow and reach groundwater and surface water sources, becoming a latent danger in drinking water. Hence, due to the inefficiency of conventional wastewater treatment technologies, wastewater enters the environment through the output effluent. In recent years, this trend has caused growing concerns regarding the presence of various pharmaceutical materials in water [19-23,4]. Among these pharmaceutical contaminants, anti-cancer medicines are classified according to their mechanism of action, including factors affecting DNA, anti-metabolism, hormones and antagonists, molecular targeting agents, monoclonal antibodies, and biological agents. Among anticancer medicines, PTX and GEM are used to treat certain types of cancerous tumors, such as advanced bile duct, breast, and lung cancer [24]. The presence of these substances in the effluent, even at low concentrations, poses highly dangerous problems such as mutagenic, cytotoxic, genotoxic, and carcinogenic effects for humans and other living organisms. Since it is difficult to remove pharmaceutical contaminants, the probability of the simultaneous presence of these harmful compounds in the effluents of pharmaceutical plants and hospitals is strong [25,26] (Table 1). Traditional wastewater treatment methods like activated sludge are insufficient to completely remove active pharmaceutical compounds and other wastewater compounds from water. Consequently, complementary treatment methods such as

advanced oxidation [27], membrane filtration [1], reverse osmosis [28], and activated carbon are often used for industrial wastewater treatment. Adsorption is a highly effective way to remove contaminants from water and wastewater even at concentrations lower than one milligram per liter. Compared to other methods, it is a simple, inexpensive, and applicable method. Carbon nanotubes are unique macromolecules with high heat and chemical resistance [29]. Therefore, many researchers have focused on optimizing the adsorption process and finding new attractions with high adsorption capacity and low cost. Carbon nanotubes are among these adsorbents. Carbon nanotubes are graphite sheets wrapped in the form of cylindrical tubes. According to the number of layers in their structure, they are divided into two groups: single-walled carbon nanotubes (MWCNTs) and multiple walled carbon nanotubes (SWCNTs) [30-32]. In recent years, the use of multi-walled carbon nanotubes as adsorbents to remove dye from aqueous solutions has attracted the attention of researchers. Multi-walled carbon nanotubes have become effective adsorbents for dye removal owing to their exceptional properties, such as small size, a hollow structure of layers, and large specific surface area [33]. However, one of the serious challenges in using this type of adsorbent is the problem of separating carbon nanotubes from aqueous solutions and the pollution caused by their residue. The preparation of magnetic nanocomposites of multi-walled carbon nanotubes is an effective way to overcome the problem of their separation from aqueous solutions, allowing the treatment of large volumes of water contaminated by dye by applying an external magnetic field without secondary pollution [34]. In addition, the combination of the unique properties of iron oxide nanoparticles with the surface properties of multi-walled carbon nanotubes improves the adsorption capacity and increases the reaction kinetics [35]. According to published studies, thus far, no research has compared the effect of the adsorption of PTX and GEM using magnetic multi-walled carbon nanotube adsorbents. Therefore, the present study aimed to fabricate and characterize the adsorbent of the magnetic multi-walled carbon nanotubes

using the co-precipitation method and compare its performance in the adsorption of PTX and GEM.

## 2. Materials and methods

### 2.1. Chemicals and devices

The commercial multi-walled carbon nanotubes (98% purity, outer diameter of 20–30 nm, length of 10–30  $\mu\text{m}$ , specific surface area of 110  $\text{m}^2/\text{g}$ ) synthesized by the chemical vapor deposition (CVD) method were prepared by the Nanosany Corporation. Additionally, iron chloride ( $\text{FeCl}_2 \cdot 4\text{H}_2\text{O}$ ), ferric chloride ( $\text{FeCl}_3 \cdot 6\text{H}_2\text{O}$ ), hydrochloric acid (HCl, 37%), nitric acid, sulfuric acid ( $\text{H}_2\text{SO}_4$ ), ammonia solution ( $\text{NH}_4\text{OH}$ ), and ethanol were purchased from the Merck Co., Germany. Millipore's Milli-Q Advantage A10 (made in the United States) was used to prepare pure distilled water. The pH of the solutions was measured using a Metrohm pH meter, Model 713. PTX and GEM were purchased from BDR and Cipla Pharmaceuticals Co. (India). The main properties of GEM and PTX are manifest in Table 1.

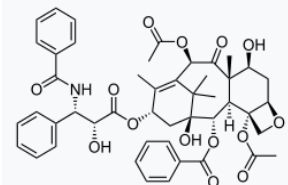
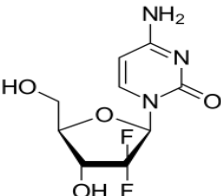
### 2.2. Preparation of $\text{Fe}_3\text{O}_4/\text{MWCNT}$ nano-adsorbents

Before the iron nanoparticles were imprinted, the carbon nanotubes were acid-washed to remove any impurities from their surfaces [36]. The carbon nanotubes were added to a solution of concentrated nitric acid and sulfuric acid (1: 1) and kept at 60°C for three hours in an ultrasonic device. It was then washed several times with ethanol and distilled water to bring the pH to normal conditions and then dried in an oven at 110°C. The co-precipitation method was used to prepare Table 1. Specifications of the studied drug sewage [37,38].

$\text{Fe}_3\text{O}_4/\text{MWCNT}$  nanoparticles. Moreover, 0.1 g of MWCNT was immersed in 50 ml of a distilled water solution containing 0.15 g of iron chloride, 0.45 g of ferric chloride, and 0.85 g of hydrochloric acid for 30 minutes in an ultrasonic water bath at 80 °C. Before reaching ambient temperature, 1 ml of 8 M ammonia solution was slowly added to the solution to adsorb the iron onto the carbon nanotube. Finally, the precipitate was adsorbed by a magnet at room temperature and washed several times with distilled water. The adsorbent was dried in a nitrogen atmosphere.

### 2.3. Characterization

The obtained nano-adsorbent morphology was evaluated by a field emission scanning electron microscope (TESCAN, Czech Republic) and a transmission electron microscope (100CX-II) at 100 kV. In addition, the crystal structure of the magnetic carbon nanotubes was investigated using the X-ray diffraction analysis (Siemens D5000, Germany). X-ray energy dispersive spectroscopy (EDS) was used to analyze elemental composition. Three spots were chosen for EDX analysis. Vibrating sample magnetometer analysis (VSM, VersaLab) was used to investigate the magnetic properties of the nano-adsorbent. A UV-Vis spectrometer (Rayleigh, UV-2601 UV-VIS, China) was used to measure the absorption capacity. The chromatographic data were performed at 270 and 227 wavelengths by injecting 20  $\mu\text{l}$  of the solution. The magnetic stirrer (IKA RH basic2, German) was used to stir the solutions, and a 1/4 Tesla magnet was used to separate the magnetic adsorbent from the solutions.

Maximum wavelength (nm)	Molecular weight (g/mol)	chemical formula	Chemical structure	Name
227	853.906	$\text{C}_{47}\text{H}_{51}\text{NO}_{14}$		(Paclitaxel)
269	263.198	$\text{C}_9\text{H}_{11}\text{F}_2\text{N}_3\text{O}_4$		(Gemcitabine)

## 2.4. Adsorption experiments

Several experiments were conducted to compare the adsorption efficiencies of the synthesized magnetic adsorbent in removing PTX and GEM. In these experiments, 50 mg of the synthesized adsorbent was placed into a reactor containing 250 ml of ethanol solvent with contaminant to equilibrate at ambient temperature and a pH of 5. At different intervals, a small amount of the contaminant solution without adsorbent was sampled for spectroscopic examination. These experiments were performed separately for different concentrations of PTX and GEM (between 5 and 50 mg/L). The maximum wavelengths for PTX and GEM were 227 and 269, respectively. The calibration diagram was obtained by considering different concentrations of contaminants. Furthermore, a darkness test was conducted without the addition of an adsorbent to determine if the contaminant concentration changed over time. Isotherm and adsorption kinetics were also calculated.

## 3. Results and discussion

### 3.1. Determination of the morphology of magnetic carbon nanotubes

The morphology of  $\text{Fe}_3\text{O}_4/\text{MWCNT}$  nanoparticles was investigated using the FESEM and TEM images.

The FESEM image in Figure 1 depicts the morphology of the surface of the particles constituting the magnetic composite. The FESEM image shows that the multi-walled carbon nanotubes retained their tubular structure after the magnetization process. The TEM image indicates that the iron oxide nanoparticles (darker spots) were uniformly inoculated on the surface of the nanotubes. The reason for this phenomenon was that the electrostatic force between the positive charge of the  $\text{Fe}_3\text{O}_4$  surface and the negative charge of the nanotube surface prevented severe aggregation and closing of the nanotube cavities.

### 3.2. EDX analysis

An energy-dispersive X-ray spectrometer (EDS) was used to examine the microstructure of the  $\text{Fe}_3\text{O}_4/\text{MWCNT}$  composite. As illustrated in Figure 2, the carbons exhibit a tube-shaped structure. Moreover, Fig. 2 depicts the corresponding EDX spectrum of samples, confirming the presence of carbon and iron elements in synthesis samples. The absorption peak at 6.5 keV in the EDX spectrum of doped samples is indexed to metallic Fe, while the absorption peak at 0.277 keV is indexed to carbon. The quantitative elemental composition of  $\text{Fe}_3\text{O}_4/\text{MWCNT}$  samples is summarized in Table 2.

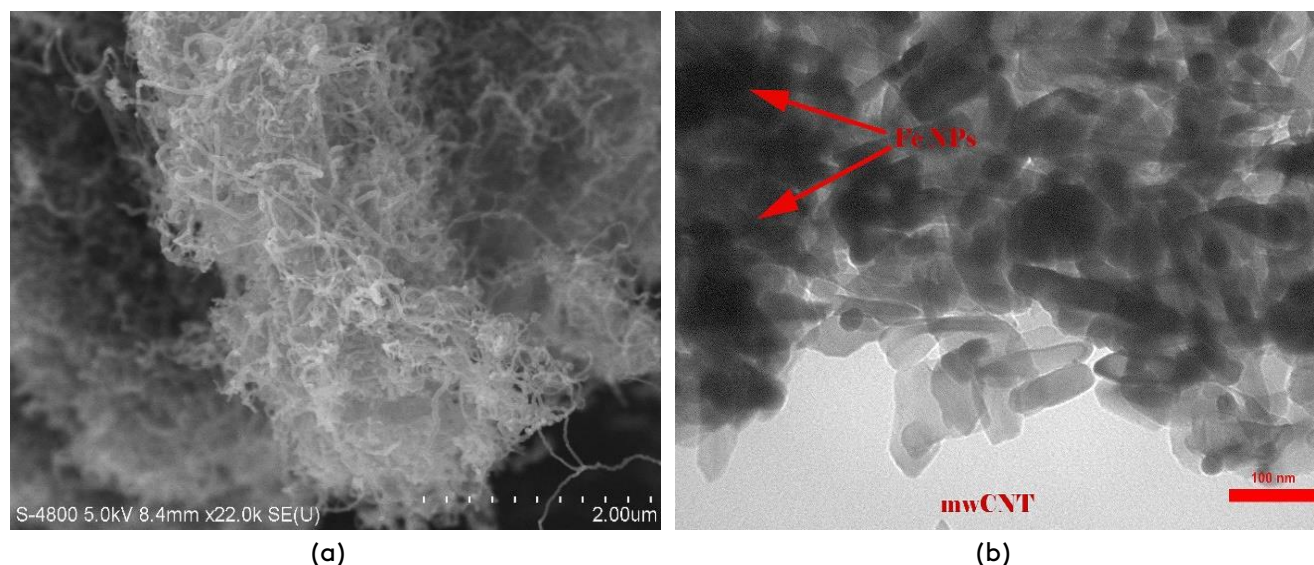


Fig. 1. Images (a) FESEM and (b) TEM related to adsorbent of multi-walled magnetic carbon nanotubes.

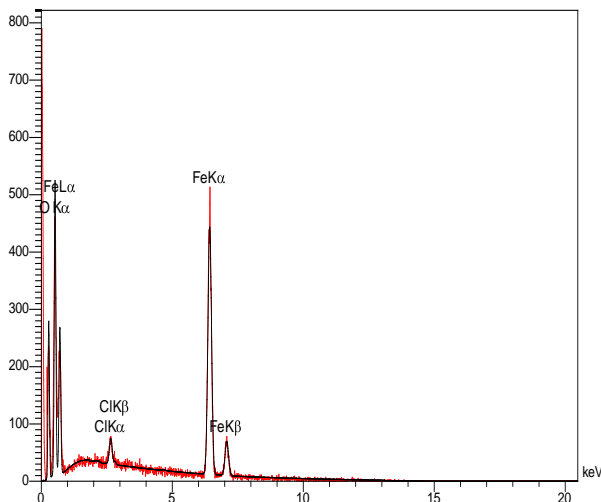


Fig. 2. EDX spectra of  $\text{Fe}_3\text{O}_4/\text{MWCNT}$  sample.

Table 2. Elemental chemical analysis of the prepared samples.

Sample	C (w%)	O (w%)	Fe (w%)	Cl (w%)
$\text{Fe}_3\text{O}_4/\text{MWCNT}$	70.24	3.69	25.51	0.56

### 3.3. The structural analysis of the $\text{Fe}_3\text{O}_4/\text{MWCNT}$ adsorbent

Figure 3 (a) shows the X-ray diffraction pattern for pure and magnetized nanotubes. The peaks in the positions of  $26.18^\circ$  and  $46.49^\circ$  with Miller indices (002) and (100) were related to multi-walled carbon nanotubes. The crystal diffractions in the positions of  $33.74^\circ$ ,  $37.25^\circ$ ,  $45.09^\circ$ ,  $59.09^\circ$ , and  $62.67^\circ$  with the Miller indices (220), (311), (400), (422), and (440), respectively, were related to iron oxide molecules [39]. The results of the X-ray diffraction pattern analysis indicated that the method used resulted in the formation of carbon magnetic nanocomposites by creating the least amount of impurities in the crystal structure. Fig. 3 (b) shows the vibrating sample magnetometer of

the curve synthesized nano-adsorbent. According to the figure, the  $\text{Fe}_3\text{O}_4/\text{MWCNT}$  nano-adsorbent had a high saturated magnetic property (39.2 emu/g). This amount of magnetic property caused the nano-adsorbent to be completely absorbed and separated by an external magnetic field. This property will increase the adsorption capacity and allow the easier recovery and separation of the adsorbent from the effluent. Figure 4 shows a diagram of the adsorption of GEM and PTX solutions by the  $\text{Fe}_3\text{O}_4/\text{MWCNT}$  magnetic adsorbent. GEM and PTX solutions with a concentration of 50 mg/L were mixed with ethanol solvent using a magnetic stirrer. This was carried out in a dark environment to prevent the effect of light radiation on the adsorption process. As Figure 4 shows, after one hour, the adsorption process was in equilibrium. Based on the results, the magnetic multi-walled carbon nanotube adsorbent adsorbed PTX well into the effluent solution, while a small percentage of GEM was adsorbed. The percentage of PTX removal after one hour was 58%, while this number was 26% for GEM. For the above experiments, the removal efficiency (R) and adsorption capacity ( $q_e$ ) are represented by Equation (1) and Equation (2), respectively [40].

$$R (\%) = \frac{(C_0 - C_e)}{C_0} * 100\% \quad (1)$$

$$q_e = \frac{(C_0 - C_e) V}{m} \quad (2)$$

where  $C_0$  (mg/L) represents the paclitaxel and gemcitabine concentration before adsorption;  $C_e$  (mg/L) represents the PTX and GEM concentration after adsorption;  $m$  (g) represents the dosage of  $\text{Fe}_3\text{O}_4/\text{MWCNT}$ ;  $V$  (mL) represents the volume of solution.



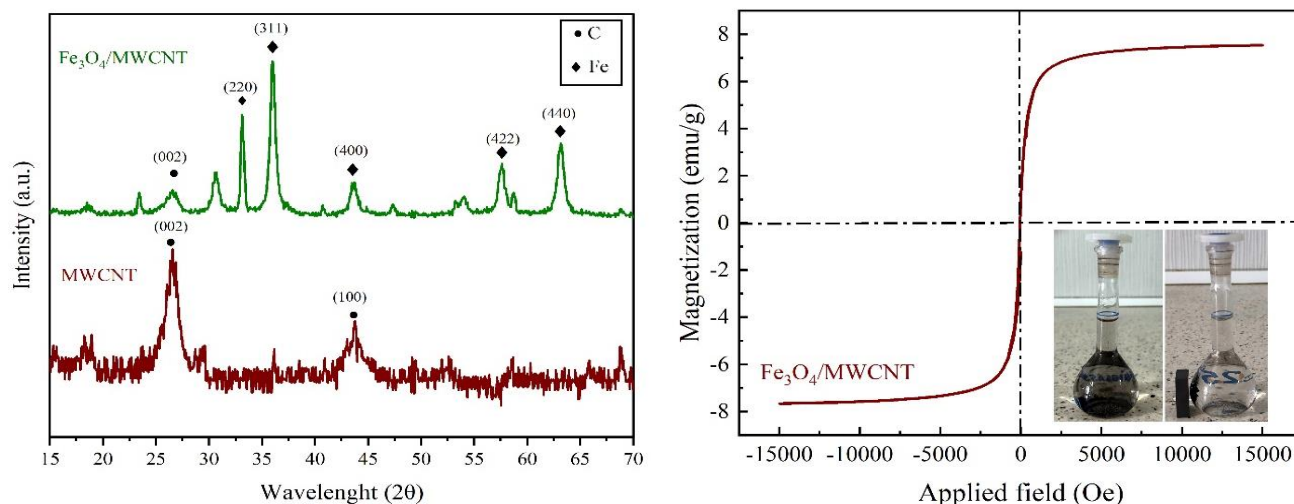


**Fig. 3.** (a) Diagram of XRD analysis of pure and magnetic multi-walled carbon nanotubes, b) VSM curve of magnetized sample.

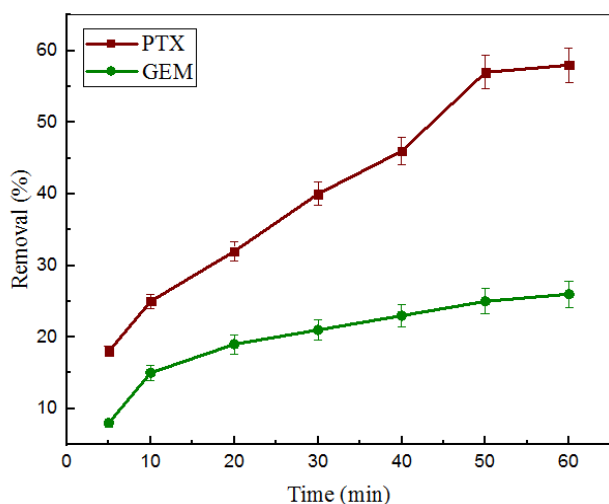


**Fig. 4.** Adsorption diagram of GEM and PTX solutions by magnetic adsorbent  $\text{Fe}_3\text{O}_4 / \text{MWCNT}$  (at pH 7, adsorbent dose 200 mg/L, and initial contaminant concentration 50 mg/L).

### 3.4. The effect of solution pH on removal efficiency

The pH of the solution plays a crucial role in the adsorption process. Adsorption properties change by changing the pH value of the adsorbent surface charge and the degree of ionization. In the present study, to evaluate the effect of pH on the adsorption process, equilibrium experiments were conducted at a different range of pH 3-11. The pH was adjusted by concentrated HCL and NaOH solutions. The normal pH of the GEM and PTX solutions was 3.1 and 3.7, respectively. Fig 5 shows that the pH value has a considerable effect on the adsorption capacity of the adsorbent in the PTX solution; however, in the GEM solution, it has a

minimal effect. From pH 3 to 7, the adsorption capacity of the PTX solution increased, and at pH 11, the percentage of PTX removal decreased sharply. The cause of this phenomenon is related to the positive charge of PTX molecules and the creation of electrostatic repulsion, which is related to the interaction of the  $\pi$ - $\pi$  bond between the PTX benzene ring and carbons [16]. However, changes in the percentage of GEM removal in this pH range were slight and fluctuated. The maximum amount of adsorption still occurred at a pH between 7 and 7.5. In addition, the absorption capacity of GEM also decreased sharply at pH 11.

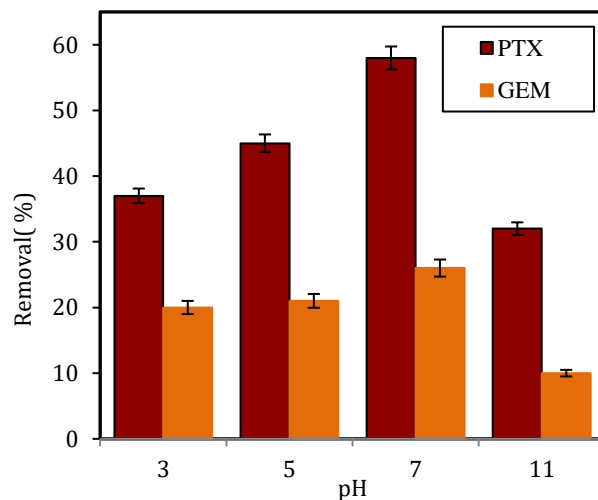


**Fig. 5.** Changes in the removal percentage of paclitaxel and gemcitabine at different pH.

### 3.5. The effect of the $\text{Fe}_3\text{O}_4/\text{MWCNT}$ dosage on the removal efficiency of GEM and PTX

As a fact, the concentration of any adsorbent can potentially affect its removal efficiency. In the present study, different concentrations of  $\text{Fe}_3\text{O}_4/\text{MWCNT}$  (25, 50, 100, 150, 200 and 250 mg) were examined to find the optimum dosage in which the highest adsorption of GEM and PTX occurred. The experiments were carried out at the initial concentration of 50 mg/L GEM and PTX, a contact time of 60 min, and under a pH condition of 7 (Figure 6). According to obtained results (Figure 6), by increasing the adsorbent concentration from 25 to 200 mg, the adsorption of GEM and PTX increased. According to the figure, an increase in the carbon nanotube dosage had a significant effect on the removal of GEM and PTX (the removal percentage of PTX increased to 85.28% and GEM to 60.8%). And then a decrease was observed. This clearly showed that by increasing the adsorbent dose, more active sites were ready to adsorb paclitaxel and gemcitabine from the solution until the saturation of the nanotube [41]. The efficiency was augmented by increasing the  $\text{Fe}_3\text{O}_4/\text{MWCNT}$  from 25 to 200 mg/L, and the 200 mg/L of carbon nanotube had the highest removal efficiency, so it was used in the following steps.

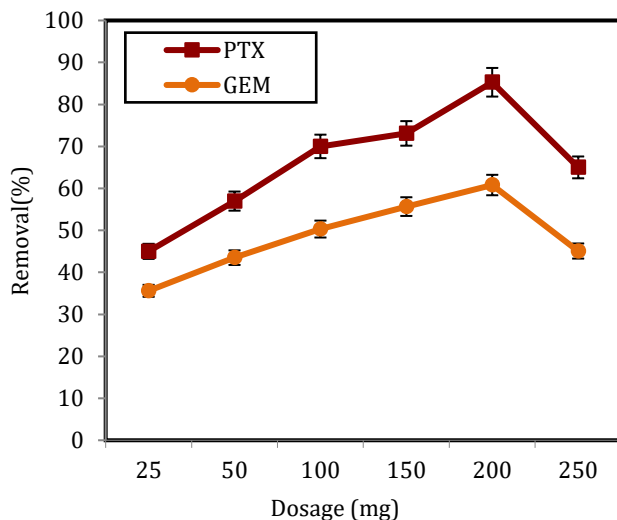


**Fig. 6.** The effect of adsorbent dosage on the efficiency of GEM and PTX removal (Conditions: pH 7, initial GEM and PTX concentration of 50 mg/L, and contact time of 30 min).

### 3.6. Adsorption kinetics

Chemical kinetics indicate the speed of chemical reactions. In the present research, the adsorption rate constants of GEM and PTX by magnetic multi-walled carbon nanotubes were matched with quasi-first and quasi-second kinetic models and the most suitable model was determined. For this evaluation, Equation 3 was used:

$$\frac{dC}{dt} = -kq_e^n \quad (3)$$

In this equation,  $q_e$  is the equilibrium concentration of the adsorbent phase in the soluble mass at time  $t$ ,  $k$  is the reaction rate constant, and  $n$  is the reaction degree. To evaluate the order of degradation kinetics by placing the values  $n = 1, 2$  in the above relation and differentiation, the following relations will be obtained [42, 43].

$$n = 1 \rightarrow \ln(q_e - q_t) = \ln q_e - k_1 t \quad (4)$$

$$n = 2 \rightarrow \frac{t}{q_t} = \frac{1}{k_2 q_e^2} + \frac{t}{q_e} \quad (5)$$

where  $q_e$  and  $q(t)$  are the amount of absorption (mg/g) at equilibrium and  $t$  time, respectively;  $k_1$  and  $k_2$  are the first- and second-order reaction rate constants, respectively. The linear curves of concentration versus time are plotted for all the reaction degrees at different concentrations of 5, 25, and 50 mg/L. Table 2 presents the results of the values of its linear correlations. Figure 7 depicts the effect of the first- and second-order kinetics of the initial concentrations of PTX and GEM on it. The pseudo-first-order kinetic model is based on the assumption that the rate of change of solute uptake with time is directly proportional to the difference in saturation concentration and the amount of solid uptake with time. The quasi-second order model assumes that two reactions (parallel or series) affect the adsorption of the material, and the parallel reaction equilibrates rapidly, while the series reaction has a slow velocity and lasts longer [13]. Finally, the degree of reaction is estimated by comparing the values of the linear correlations obtained. The results showed that by comparing the correlation coefficients of different degrees of reaction for each sample, the curve fitting the correlation coefficient was higher in the second-order equation. The kinetic data indicated that the absorption of PTX and GEM contaminants

was faster at the beginning of the process and was fixed over time. Various mechanisms control the adsorption kinetics, the most important limiting

factors of which are infiltration mechanisms, such as external infiltration, boundary layer infiltration, and intermolecular infiltration [44].

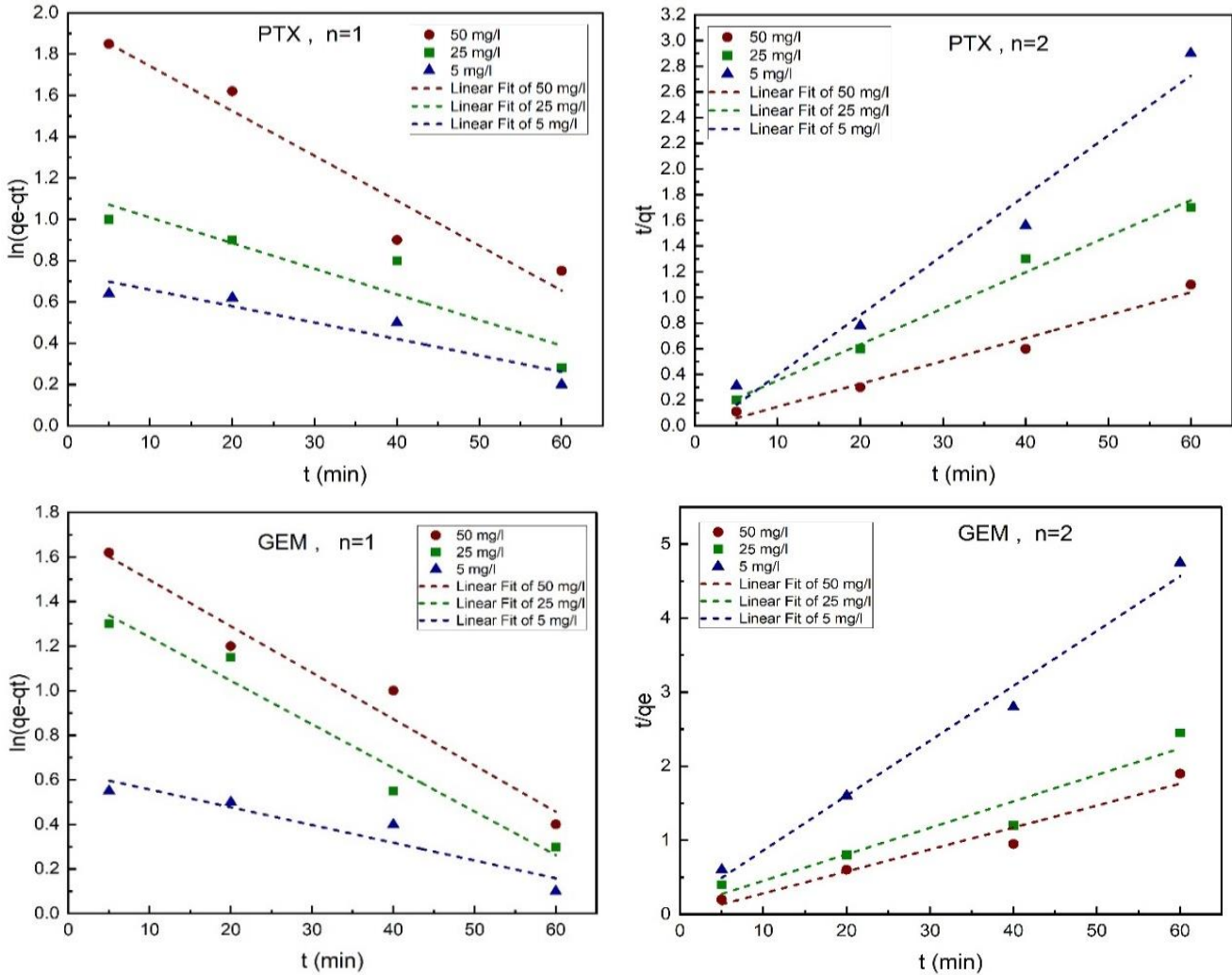


Fig. 7. Matching diagrams of the results of the first-order reaction model for a) paclitaxel and c) gemcitabine and the second-order reaction model for b) a) paclitaxel and d) gemcitabine.

Table 3. Results of fitting kinetic curves based on first and second order reactions.

Quadratic kinetics model			First class kinetics model			Concentration (mg/L)	Pollutant
$q_m$	$k_2$	$R^2$	$q_m$	$k_1$	$R^2$		
21.45	0.31	0.9705	2.09	0.0079	0.8771	5	(Paclitaxel)
35.58	0.10	0.9298	3.12	0.0124	0.8582	25	
59.88	0.013	0.9553	7.11	0.0214	0.9373	50	
13.49	0.044	0.9868	1.88	0.0080	0.9646	5	(Gemcitabine)
28.01	0.013	0.9887	4.20	0.0196	0.9638	25	
32.67	0.035	0.9543	5.50	0.0201	0.9371	50	



### 3.7. Investigation of adsorption isotherms

To analyze the results of adsorption and its isotherms, the Langmuir and Freundlich models were investigated. The linear equations of Langmuir (6) and Freundlich (7) were used to fit the absorption curve [45].

$$\frac{C_e}{q_e} = \frac{C_e}{q_m} + \frac{1}{K_L q_m} \quad (6)$$

$$\log(q_e) = \log(K_F) + \left(\frac{1}{n}\right) \log(C_e) \quad (7)$$

In the above relations,  $C_e$  (mg/L) and  $q_e$  (mg/g) show the equilibrium concentration in the soluble and solid phases, respectively,  $q_m$  (mg/g) is the maximum adsorption capacity, and  $K_L$  (mg/L) is the value of nonlinearity. The important property in the Langmuir isotherm is determined by the dimensionless equilibrium parameter ( $R_L$ ), which is defined as follows:

$$R_L = \frac{1}{1 + K_L C_0} \quad (8)$$

where  $C_0$  (mg/L) is the highest initial concentration of adsorption, and  $R_L$  indicates that the isotherm is undesirable ( $R_L > 1$ ), linear ( $R_L = 1$ ),

desirable ( $0 < R_L < 1$ ) or irreversible ( $R_L = 0$ ). Langmuir and Freundlich isotherm models are widely used to evaluate the adsorption process. The Langmuir isotherm is based on single layer adsorption into a certain number of active sites. In this model, it is assumed that adsorption occurs in places with the same energy on the adsorbent surface, while in the Freundlich isotherm, the soluble substance is adsorbed on dissimilar surfaces and in several layers [43]. The absorption diagrams determined by the Langmuir and Freundlich equations are shown in Fig. 8, and the coefficients and constants of each are presented in Table 4. The linear regression coefficients of the Langmuir adsorption were 0.9158 for PTX adsorption and 0.8902 for GEM adsorption. However, the linear regression coefficients of the Freundlich adsorption isotherm were 0.8695 and 0.8052, respectively. It showed that the studied adsorption process followed the Langmuir isotherm model. Moreover, the maximum adsorption capacity of  $Fe_3O_4/MWCNT$  nano-absorbents for the PTX solution was higher than that of the GEM solution, being consistent with the adsorption results.

Table 4. Results from equilibrium data fitting to determine the isotherm.

Freundlich			Langmuir			Pollutant
$R^2$	$n$	$K_F$ (l/mg)	$R^2$	$R_L$	$K_L$ (l/mg)	
0.8695	2.5	17.832	0.9158	0.16	1046	(Paclitaxel)
0.8052	3	15.727	0.8902	0.12	89.5	(Gemcitabine)

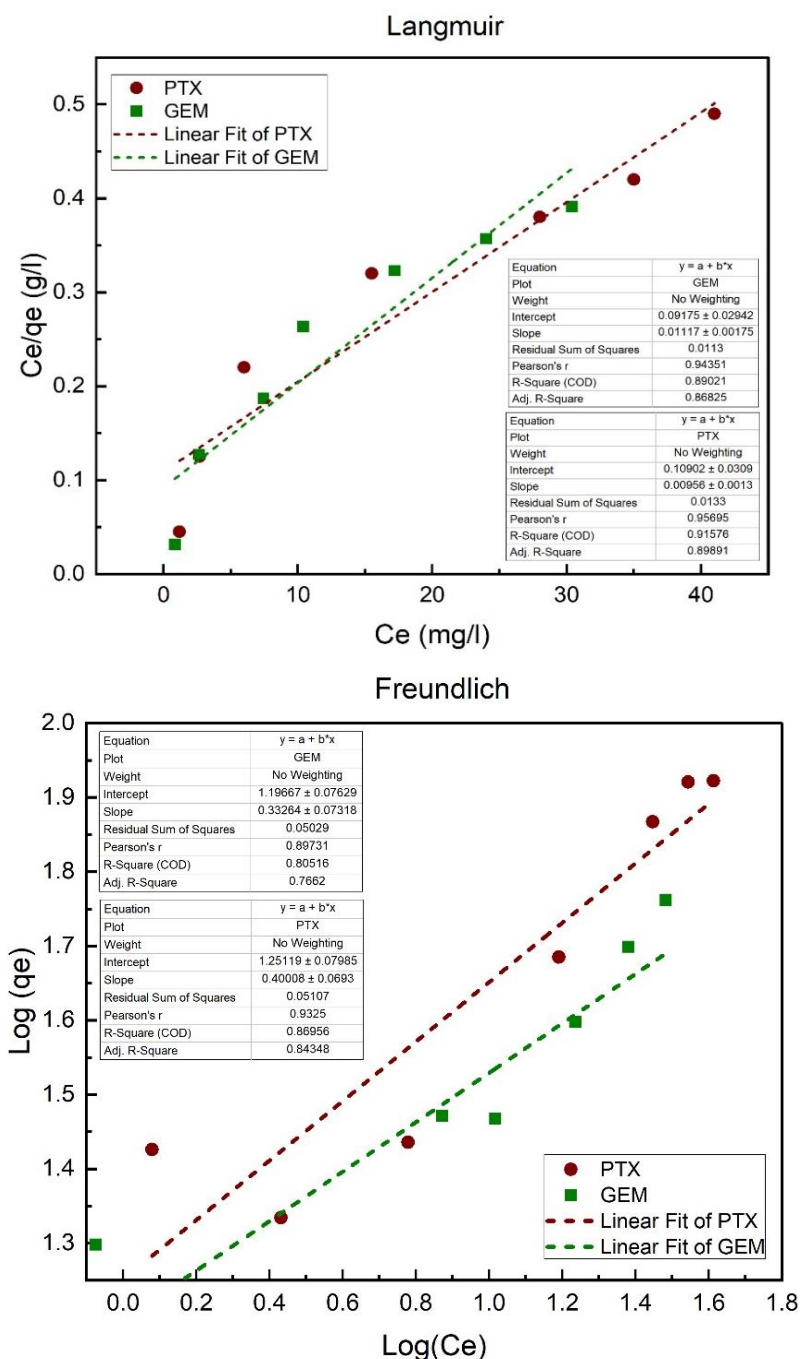


**Fig. 8.** Results of isothermal models a) Langmuir and b) Freundlich for paclitaxel effluents of Gemcitabine.

### 3.8. Recovery

Several experiments on the prepared samples were conducted to confirm the possibility of recycling the adsorbent in its prepared state. Figure 9 illustrates the stability of  $\text{Fe}_3\text{O}_4/\text{MWCNT}$  after five cycles of PTX and GEM adsorption. It should be noted that following each cycle, the adsorbent was extracted using an external magnetic force; then, it was sonicated and washed with deionized water, immersed for 10 min in ethanol, and finally dried in

an oven. As illustrated in the figure, the adsorption efficiency of PTX with  $\text{Fe}_3\text{O}_4/\text{MWCNT}$  adsorbents remained high, with a total loss of only 8%, while this number was 5% for GEM, indicating effective magnetic properties, mechanical robustness, low corrosion, and excellent chemical stability. However, the recovery rate of GEM was lower than that of PTX. This indicated that the  $\text{Fe}_3\text{O}_4/\text{MWCNT}$  could be applied in practical pharmaceutical wastewater treatment.

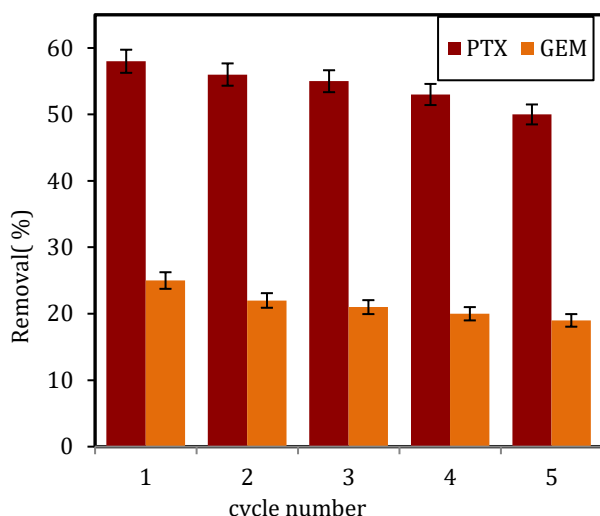


**Fig. 9.** Stability of the prepared samples after five cycles in the adsorption of PTX and GEM solution (200mg of adsorbents, 50ppm, pH=7).

## 5. Conclusions

In the present research, GEM and PTX contaminants were removed from the effluent using a multi-walled carbon nanotube magnetized by co-precipitation. The synthesized nano-adsorbents were examined using FESEM, TEM, XRD, and VSM analyses. Additionally, the adsorption performance of the multi-walled carbon nanotubes in removing GEM and PTX contaminants was compared, and the effect of the pH solution and the adsorbent dosage were investigated. Adsorption kinetics and reaction isotherms for each contaminant were also calculated, indicating that the absorption of the medicines followed a second-order reaction and the Langmuir isotherm. This study demonstrated that the efficiency of magnetic multi-walled carbon nanotubes in removing GEM from pharmaceutical effluents was lower than that of PTX. However, as magnetic carbon nanotubes can be regenerated and reused, this defect can be compensated by successive uses. Moreover, the desorption and recovery efficiencies for both drugs were determined, confirming the remarkable stability and reusability of the adsorbent. The entry of carbon nanotubes into the environment can be considerably reduced by creating an external magnetic field. Based on this study and according to the obtained results, it is suggested to check the following items to remove paclitaxel and gemcitabine in future studies:

- 1- The effect of different experimental conditions (temperature and ion concentration)
- 2- Selective separation of each of the drugs in the presence of other drugs by Fe<sub>3</sub>O<sub>4</sub>/MWNCT
- 3- Use of other nanoparticles (copper oxide, etc.)
- 4- Extraction of other cytotoxic drugs, such as cisplatin, oxaliplatin, epirubicin, etc.

## Acknowledgments

This research is extracted from the dissertation of a Ph.D. student (Ms. Setareh Safari) in Environmental Engineering, Islamic Azad University of Ardabil Branch with the dissertation code of 11948006027759973256. Therefore, the authors appreciate the esteemed president and educational and research deputies of the Ardabil Islamic Azad University for their cooperation in facilitating the implementation of this project.

## References

- [1] Homem, V., Santos, L. (2011). Degradation and removal methods of antibiotics from aqueous matrices—a review. *Journal of environmental management*, 92(10), 2304-2347.
- [2] Huang, L., Sun, Y., Wang, W., Yue, Q., Yang, T. (2011). Comparative study on characterization of activated carbons prepared by microwave and conventional heating methods and application in removal of oxytetracycline (OTC). *Chemical engineering journal*, 171(3), 1446-1453.
- [3] Mohammadi Aloucheh, R., Baris, O., Asadi, A., Gholam Zadeh, S., Kharat Sadeghi, M. (2019). Characterization of Aquatic Beetles Shells (Hydraenidae family) derived chitosan and its application in order to eliminate the environmental pollutant bacterial. *Anthropogenic pollution*, 3(2), 43-48.
- [4] Mirzade Ahari, S., Mahvi, A., Jalilzadeh Yangejeh, R., Dadban Shahamat, Y. and Takdastan, A. (2019). A new method for the removal of ammonium from drinking water using hybrid method of modified zeolites/catalytic ozonation. *Desalination and water treatment*, 170, 148-157.
- [5] Nikpour, B., Jalilzadeh Yengejeh, R., Takdastan, A., Hassani, A., Zazouli, M. (2020). The investigation of biological removal of nitrogen and phosphorous from domestic wastewater by inserting anaerobic/anoxic holding tank in

- the return sludge line of MLE-OSA modified system. *Journal of environmental health science and engineering*, 18(1), 1-10.
- [6] Gooran Ourimi, H., Nezhadnaderi, M. (2020). Comparison of the application of heavy metals adsorption methods from aqueous solutions for development of sustainable environment. *Anthropogenic pollution*, 4(2), 15-27.
- [7] Ghomi Avili, F. (2021). Removal of heavy metals (Lead and Nickel) from water sources by adsorption of activated alumina. *Anthropogenic pollution*, 5(2), 1-7.
- [8] Farsani, M. H., Yengejeh, R. J., Mirzahosseini, A. H., Monavari, M., Mengelizadeh, N. (2022). Effective leachate treatment by a pilot-scale submerged electro-membrane bioreactor. *Environmental science and pollution research*, 29(6), 9218-9231.
- [9] Kazemi Noredinvand, B., Takdastan, A., Jalilzadeh Yengejeh, R. (2016). Removal of organic matter from drinking water by single and dual media filtration: a comparative pilot study. *Desalination and water treatment*, 57(44), 20792-20799.
- [10] Kordestani, B., Yengejeh, R. J., Takdastan, A., Neisi, A. K. (2019). A new study on photocatalytic degradation of meropenem and ceftriaxone antibiotics based on sulfate radicals: Influential factors, biodegradability, mineralization approach. *Microchemical journal*, 146, 286-292.
- [11] Rivas, F., Gimeno, O., Borallho, T. (2012). Aqueous pharmaceutical compounds removal by potassium monopersulfate. Uncatalyzed and catalyzed semicontinuous experiments. *Chemical engineering journal*, 192, 326-333.
- [12] Babaei, A. A., Ghanbari, F., Yengejeh, R. J. (2017). Simultaneous use of iron and copper anodes in photoelectro-Fenton process: concurrent removals of dye and cadmium. *Water science and technology*, 75(7), 1732-1742.
- [13] Amini Fard, F., Jalilzadeh Yengejeh, R., Ghaeni, M. (2019). Efficiency of Microalgae *Scenedesmus* in the removal of nitrogen from municipal wastewaters. *Iranian journal of toxicology*, 13(2), 1-6.
- [14] Mehrdoost, A., Jalilzadeh Yengejeh, R., Mohammadi, M. K., Babaei, A. A., Haghhighatzadeh, A. (2021). Comparative Analysis of UV-assisted Removal of Azithromycin and Cefixime from Aqueous Solution Using PAC/Fe/Si/Zn Nanocomposite. *Journal of health sciences and surveillance system*, 9(1), 39-49.
- [15] Zhang, L., Song, X., Liu, X., Yang, L., Pan, F., Lv, J. (2011). Studies on the removal of tetracycline by multi-walled carbon nanotubes. *Chemical engineering journal*, 178, 26-33.
- [16] Ghanavat Amani, M., Jalilzadeh Yengejeh, R. (2021). Comparison of escherichia coli and klebsiella removal efficiency in aquatic environments using silver and copper nanoparticles. *Journal of health sciences and surveillance system*, 9(2), 72-80.
- [17] Ebadi, M., Asareh, A., Jalilzadeh Yengejeh, R., Hedayat, N. (2021). Investigation of Electro-coagulation Process for Phosphate and Nitrate Removal From Sugarcane Wastewaters. *Iranian journal of toxicology*, 15(1), 19-26.
- [18] Ofiarska, A., Pieczyńska, A., Borzyszkowska, A. F., Stepnowski, P., Siedlecka, E. M. (2016). Pt-TiO<sub>2</sub>-assisted photocatalytic degradation of the cytostatic drugs ifosfamide and cyclophosphamide under artificial sunlight. *Chemical engineering journal*, 285, 417-427.
- [19] Heberer, T. (2002). Occurrence, fate, and removal of pharmaceutical residues in the aquatic environment: a review of recent research data. *Toxicology letters*, 131(1-2), 5-17.
- [20] Kordestani, B., Takdastan, A., Jalilzadeh Yengejeh, R., Neisi, A. K. (2020). Photo-Fenton oxidative of pharmaceutical wastewater containing meropenem and ceftriaxone antibiotics: influential factors, feasibility, and biodegradability studies. *Toxin reviews*, 39(3), 292-302.
- [21] Shokri, R., Yengejeh, R. J., Babaei, A. A., Derikvand, E., Almasi, A. (2019). UV activation of hydrogen peroxide for removal of azithromycin antibiotic from aqueous solution: determination of optimum conditions by response surface methodology. *Toxin Reviews*, 39(3), 284-291.
- [22] Shokri, R., Jalilzadeh Yengejeh, R., Babaei, A. A., Derikvand, E., Almasi, A. (2020). Advanced

- Oxidation Process Efficiently Removes Ampicillin from Aqueous Solutions. *Iranian journal of toxicology*, 14(2), 123-130.
- [23] Zangeneh, A., Sabzalipour, S., Takdatsan, A., Yengejeh, R. J., Khafaie, M. A. (2021). Ammonia removal from municipal wastewater by air stripping process: An experimental study. *South african journal of chemical engineering*, 36, 134-141.
- [24] Rowinsky, E. K., Cazenave, L. A., Donehower, R. C. (1990). Taxol: a novel investigational antimicrotubule agent. *JNCI: Journal of the national cancer institute*, 82(15), 1247-1259.
- [25] Jureczko, M., Kalka, J. (2020). Cytostatic pharmaceuticals as water contaminants. *European journal of pharmacology*, 866, 172816.
- [26] Yousefi, M., Rahmani, K., Jalilzadeh Yengejeh, R., Sabzalipour, S., Goudarzi, G. (2021). Green synthesis of zero Iron nanoparticles and its application in the degradation of metronidazole. *Journal of health sciences and surveillance system*, 9(1), 66-70.
- [27] Veloutsou, S., Bizani, E., Fytianos, K. (2014). Photo-Fenton decomposition of  $\beta$ -blockers atenolol and metoprolol; study and optimization of system parameters and identification of intermediates. *Chemosphere*, 107, 180-186.
- [28] Urriaga, A., Pérez, G., Ibáñez, R., Ortiz, I. (2013). Removal of pharmaceuticals from a WWTP secondary effluent by ultrafiltration/reverse osmosis followed by electrochemical oxidation of the RO concentrate. *Desalination*, 331, 26-34.
- [29] Madrakian, T., Afkhami, A., Ahmadi, M., Bagheri, H. (2011). Removal of some cationic dyes from aqueous solutions using magnetic-modified multi-walled carbon nanotubes. *Journal of hazardous materials*, 196, 109-114.
- [30] Sheng, G., Shao, D., Ren, X., Wang, X., Li, J., Chen, Y., Wang, X. (2010). Kinetics and thermodynamics of adsorption of ionizable aromatic compounds from aqueous solutions by as-prepared and oxidized multiwalled carbon nanotubes. *Journal of hazardous materials*, 178(1-3), 505-516.
- [31] Gashtasbi, F., Yengejeh, R. J., Babaei, A. A. (2017). Adsorption of vancomycin antibiotic from aqueous solution using an activated carbon impregnated magnetite composite. *Desalination and water treatment*, 88, 286-297.
- [32] Gashtasbi, F., Yengejeh, R. J., Babaei, A. A. (2018). Photocatalysis assisted by activated-carbon-impregnated magnetite composite for removal of cephalexin from aqueous solution. *Korean journal of chemical engineering*, 35(8), 1726-1734.
- [33] Tasis, D., Tagmatarchis, N., Bianco, A., Prato, M. (2006). Chemistry of carbon nanotubes. *Chemical reviews*, 106(3), 1105-1136.
- [34] Sivashankar, R., Sathya, A., Vasantharaj, K., Sivasubramanian, V. (2014). Magnetic composite an environmental super adsorbent for dye sequestration—A review. *Environmental nanotechnology, monitoring and management*, 1, 36-49.
- [35] El-Sheikh, A. H., Qawariq, R. F., Abdelghani, J. I. (2019). Adsorption and magnetic solid-phase extraction of NSAIDs from pharmaceutical wastewater using magnetic carbon nanotubes: Effect of sorbent dimensions, magnetite loading and competitive adsorption study. *Environmental technology and innovation*, 16, 100496.
- [36] Blanchard, N. P., Hatton, R., Silva, S. R. P. (2007). Tuning the work function of surface oxidised multi-wall carbon nanotubes via cation exchange. *Chemical physics letters*, 434(1-3), 92-95.
- [37] Singla, A. K., Garg, A., Aggarwal, D. (2002). Paclitaxel and its formulations. *International journal of pharmaceuticals*, 235(1-2), 179-192.
- [38] Betsiou, M., Bantsis, G., Zoi, I., Sikalidis, C. (2012). Adsorption and release of gemcitabine hydrochloride and oxaliplatin by hydroxyapatite. *Ceramics international*, 38(4), 2719-2724.
- [39] FAN, X.-j., Xin, L. (2012). Preparation and magnetic property of multiwalled carbon nanotubes decorated by Fe<sub>3</sub>O<sub>4</sub> nanoparticles. *New carbon materials*, 27(2), 111-116.
- [40] Zhao, P., Geng, T., Zhao, Y., Tian, Y., Li, J., Zhang, H., Zhao, W. (2021). Removal of Cu (II) ions from aqueous solution by a magnetic multi-wall carbon nanotube adsorbent.



- Chemical engineering journal advances*, *8*, 100184.
- [41] Samadi, M. T., Shokoohi, R., Araghchian, M., & Tarlani Azar, M. (2014). Amoxicillin Removal from Aquatic Solutions Using Multi-Walled Carbon Nanotubes. *Journal of Mazandaran university of medical sciences*, *24*(117), 103-115.
- [42] Zhao, W., Tian, Y., Chu, X., Cui, L., Zhang, H., Li, M., & Zhao, P. (2021). Preparation and characteristics of a magnetic carbon nanotube adsorbent: Its efficient adsorption and recoverable performances. *Separation and purification technology*, *257*, 117917.
- [43] Zhu, H., Jiang, R., Xiao, L., Zeng, G. (2010). Preparation, characterization, adsorption kinetics and thermodynamics of novel magnetic chitosan enwrapping nanosized  $\gamma$ - $\text{Fe}_2\text{O}_3$  and multi-walled carbon nanotubes with enhanced adsorption properties for methyl orange. *Bioresource technology*, *101*(14), 5063-5069.
- [44] Özcan, A., Öncü, E. M., Özcan, A. S. (2006). Adsorption of Acid Blue 193 from aqueous solutions onto DEDMA-sepiolite. *Journal of hazardous materials*, *129*(1-3), 244-252.
- [45] Ncibi, M. C., Sillanpää, M. (2015). Optimized removal of antibiotic drugs from aqueous solutions using single, double and multi-walled carbon nanotubes. *Journal of hazardous materials*, *298*, 102-110.